NANO LETTERS

Letter

pubs.acs.org/NanoLett

Mechanical Strength of Nanoporous Graphene as a Desalination Membrane

David Cohen-Tanugi and Jeffrey C. Grossman*

Department of Materials Science and Engineering, Massachusetts Institute of Technology, 77 Massachusetts Avenue, Cambridge, Massachusetts 02139, United States

Supporting Information

ABSTRACT: Recent advances in the development of nanoporous graphene (NPG) hold promise for the future of water supply by reverse osmosis (RO) desalination. But while previous studies have highlighted the potential of NPG as an RO membrane, there is less understanding as to whether NPG is strong enough to maintain its mechanical integrity under the high hydraulic pressures inherent to the RO desalination process. Here, we show that an NPG membrane can maintain its mechanical integrity in RO but that the choice of substrate for graphene is critical to this performance. Using molecular dynamics simulations and continuum fracture mechanics, we show that an appropriate substrate with openings smaller than 1 μm would allow NPG to withstand pressures exceeding 57 MPa (570 bar) or ten times more than typical pressures for seawater RO. Furthermore, we demonstrate that NPG membranes exhibit an unusual mechanical behavior in which greater porosity may help the membrane withstand even higher pressures.

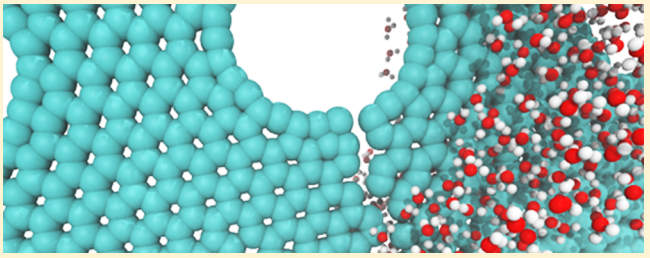

KEYWORDS: *Graphene, membrane, mechanical properties, molecular dynamics, desalination, fracture mechanics, stress intensity factor, reverse osmosis*

Desalination is the process of producing fresh water from a saline feed such as oceans or brackish sources. In an era of rapidly increasing water scarcity, desalination is expected to play a critical role in the future of the global water supply.[1] However, the viability of desalination is currently limited by large energy requirements and high capital costs relative to conventional water supply options.[2] Several studies have recently highlighted the potential of nanoporous graphene (NPG) as a next-generation membrane for reverse osmosis (RO) desalination that could dramatically enhance the access to fresh water.[2−4] With nanopores that are narrow enough to reject salt ions but large enough to allow water molecules to pass through, NPG could exhibit far greater water permeability than the RO membrane materials that are commercially in use today. Recently it was shown that increasing the permeability of RO membranes by a factor of 3 would allow for a 46% reduction in energy consumption or a 63% reduction in the number of required pressure vessels at the same pressure for brackish water RO.[5]

Although graphene exhibits exceptional mechanical properties in its defect-free state, the structural resilience of nanoporous graphene has not been examined in the specific context of water desalination. In particular, it is well-known that pores tend to weaken a material by reducing its fracture strength,[6] including in graphene.[7,8] Moreover, the presence of water reduces the fracture toughness of certain materials (e.g., oxide ceramics[9]) while increasing the fracture toughness of others (e.g., dentine),[10] an important consideration given that NPG would be continually wet inside an RO membrane. Finally, as the stress in a thin membrane under pressure scales as $d^{-2/3}$, where d is the thickness of the membrane,[11] given that graphene is ∼1,000 times thinner than the polyamide layers used in conventional thin-film composite (TFC) membranes, this begs the question of whether NPG is strong enough to withstand similar pressures without fracturing. Because the RO process relies on the molecular-level separation of salt ions from water molecules, a failure at the smallest of the length scales (i.e., the ripping of nanopores) would be sufficient to undermine the entire system.

Here, we investigate the mechanical resilience of NPG as an RO membrane. We show that the maximum pressure that NPG is able to withstand depends not only on the size and spacing of the nanopores but also more critically on the radius of the pores in the substrate material.

Background. The role of RO membranes is to extract fresh water from pressurized saltwater. In conventional TFC membranes, an active layer that is typically composed of polyamide carries out the salt rejection process.[12] This active layer extends 100−200 nm in thickness and is supported by a polysulfone substrate that is significantly more porous and thicker than the active layer with cavities around 0.1−0.5 μm and an overall layer thickness around ∼100 μm.[13−15] The

Received: June 26, 2014
Revised: September 12, 2014
Published: October 30, 2014

   dx.doi.org/10.1021/nl502399y | *Nano Lett.* 2014, 14, 6171−6178

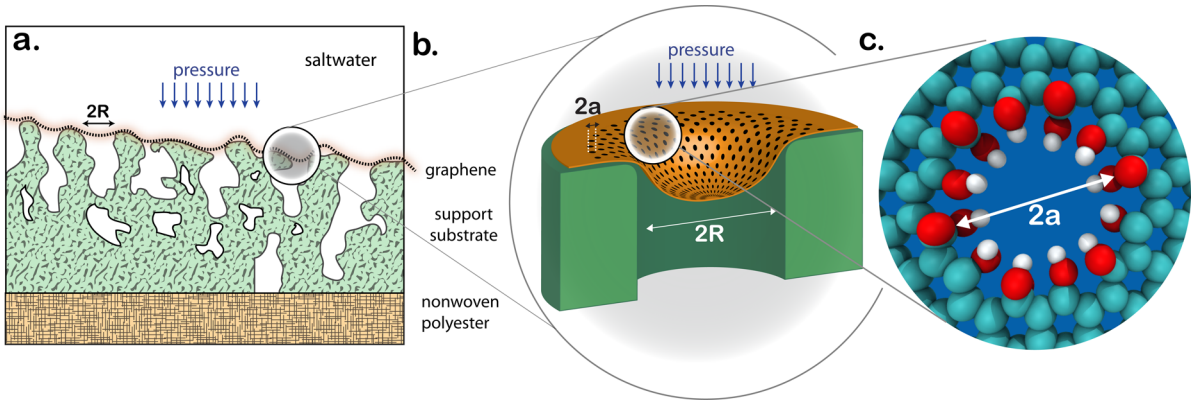

Figure 1. (a) Schematic representation of the arrangement of a nanoporous graphene (NPG) membrane. The NPG sheet is supported by a substrate with average pore radius *R*. (b) Mechanical loading on a patch of NPG due to applied pressure in an RO system. The NPG layer is approximately uniform and isotropic at the length scale of the substrate. (c) Atomic-scale visualization of NPG with nanopore radius *a*. The nanopore is shown with carboxylated edges for illustrative purposes.

primary role of the substrate is to provide a mechanical support for the active layer, bearing much of the hydraulic load while distributing the pressure from the water onto patches of active layer material. Meanwhile, the substrate plays little direct role in the salt rejection process, as water simply percolates through its pore network after permeating through the active layer.[16]

Similar to polyamide active layers, NPG must also lie atop a porous substrate (see Figure 1), although unlike TFC membranes,[14,15] design rules for the choice of the substrate material in NPG membranes are lacking. The polysulfone layer in use for conventional TFC membranes is a logical candidate, and ultrafiltration membranes with pores as narrow as 10 nm have also been employed as substrate layers for RO membranes.[17] In graphene, it has been shown that nanometer-sized pores reduce the fracture stress of the material as well as its elastic modulus.[7] It has also been shown that the maximum pressure in supported sheets of graphene decreases as a function of nanopore size and substrate pore size.[8] However, the combined role of applied pressure, membrane morphology, elastic properties, fracture stress and the effect of water have never been systematically studied. A deeper understanding of this system is necessary in order to ensure the mechanical resilience of NPG in the context of water desalination applications.

Methodology. In order to determine whether an NPG membrane will fracture at a given hydraulic pressure, we compare the stress experienced by the membrane, σ, with its fracture stress σ_f. We first determine σ_f as a function of the radius and separation of the nanopores. We then calculate σ as a function of substrate pore size and compare it with σ_f.

We simplify the problem by separating the system into two different length scales. At the micron scale, the geometrical deflection and overall mechanical response of NPG are described by continuum mechanics because each membrane patch of interest contains >100 000 carbon atoms. Macroscopic properties such as the elastic modulus, Poisson's ratio, and fracture stress are approximately isotropic at this length scale, and they dominate the mechanical behavior of NPG. In contrast, the pores in NPG play an essential role at the nanometer scale, while out-of-plane bending effects do not.[13] The mechanical loading of nanoporous graphene suspended over and adhered (i.e., clamped) at the perimeter of micrometer-sized substrate pores can be approximated using biaxial tension, as has been suggested[8] We employ clamped boundary conditions at the substrate pore perimeter, implying strong adhesion between graphene and the supporting porous material at the micrometer scale pore perimeter. Effects of slip at the substrate pore edge that may facilitate greater contributions of graphene sheet bending remain, along with considerations of more complex nanopore geometries,[8] a topic of future work.Thus, we calculate σ_f from molecular dynamics (MD) simulations and we investigate σ in NPG using continuum mechanics.

Determining the Fracture Stress of NPG. We have performed a set of MD simulations aimed at investigating precisely when and how NPG fails at the atomic scale. Following the methodology of Min and Aluru,[18] we performed stress−strain tests by enforcing a constant engineering strain rate of 0.0005 per picosecond after minimizing and equilibrating the NPG system. The strain was equibiaxial ($\varepsilon_{xx} = \varepsilon_{yy}$), and the strain increments were applied every 500 timesteps. A time step of 0.5 fs was chosen in order to ensure energy conservation and to accurately model the behavior of NPG under stress. Graphene samples were generated using VMD Nanotube Builder, and nanopores were introduced by removing atoms within a given radius of the center of the sheet, resulting in an array of NPG samples with varying pore radii and pore separations. The nanopore radii ranged from 0.2 to 1.0 nm. Functional groups at the pore edges were removed from the samples for simplicity, because we found that mechanical properties are unaffected by their presence (see Supporting Information). Because water is known to affect the fracture toughness of materials, we solvated the NPG sample in pure water using VMD Solvate[19] with ∼1 nm of water on either side. The simulations were performed using the LAMMPS molecular dynamics code (version 7.8.2013).[20] All simulations were performed in the NVT ensemble with a Nosé-Hoover thermostat at 300 K and a damping constant of 100 time steps. The simulation box contained two nanopores in each direction (for a total of four pores) with periodic boundary conditions in the *x* and *y* (planar) directions and a controllable boundary in the *z* (normal) direction. We used the AIREBO potential with a scale factor of 3.0 for the LJ interaction cutoff and both LJ and torsional terms included for graphene, and the TIP3P potential for water. The potential parameters used were ε_{CO} = 0.004423 eV, σ_{CO} = 3.188 Å, $\varepsilon_{HH} = \sigma_{HH}$ = 0.0, q_O = −0.8476 and q_H = 0.4238.[21] These parameters were derived to describe the interaction between water and the basal plane of graphitic

dx.doi.org/10.1021/nl502399y | *Nano Lett.* 2014, 14, 6171−6178

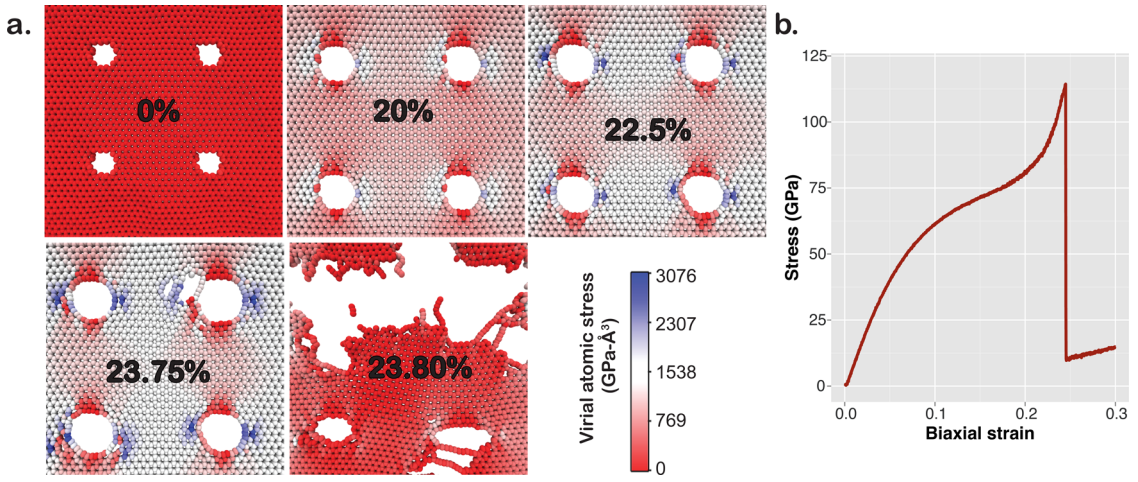

Figure 2. (a) Stress distribution in an NPG sheet (a = 0.5 nm, W = 4.0 nm) under increasing biaxial stress. The stress at each atom is represented by its color with blue regions corresponding to the areas of highest stress (see color bar). Virial atomic stresses are expressed in units of GPa-Å^3. (b) Stress−strain curve for the same NPG sample under wet conditions. The fracture stress is the maximum stress prior to failure and occurs at ∼23% strain for this case.

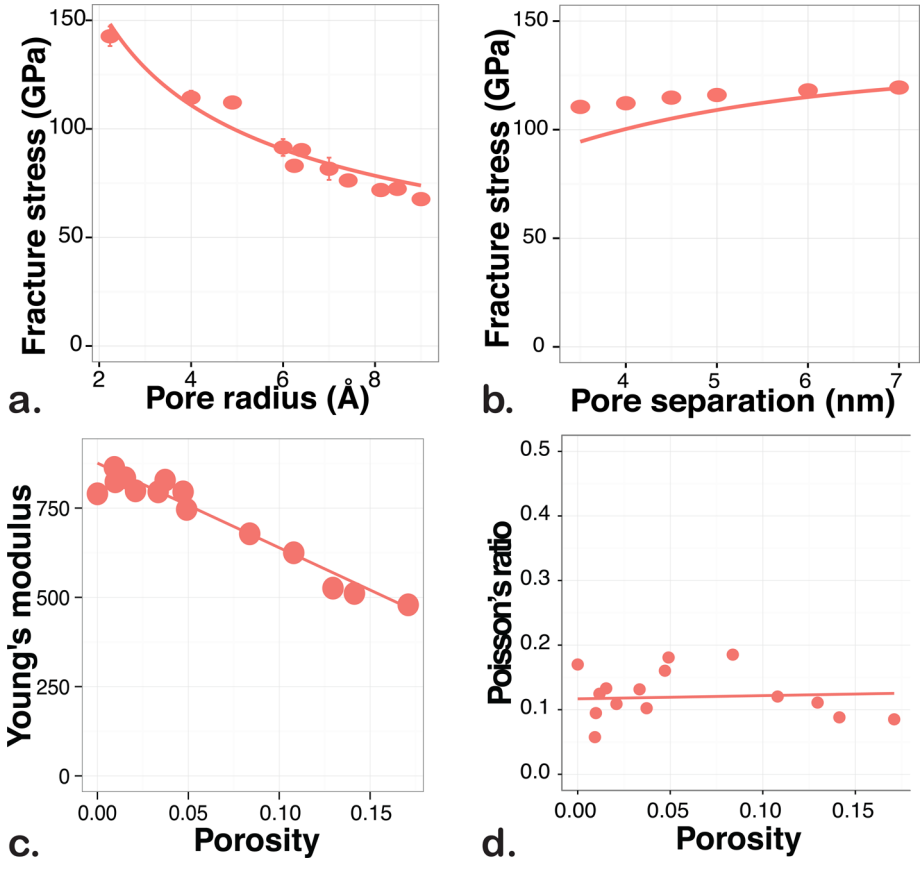

Figure 3. (a) Fracture stress as a function of nanopore radius for NPG with W = 4.0 nm under biaxial strain and submerged in water from MD simulations (b) Fracture stress as a function of nanopore separation for a = 0.5 nm. Solid lines in (a) and (b) represent the best fit for all data using eq 1. (c) Young's modulus ratio as a function of membrane porosity $p = \pi a^2/W^2$, as calculated from a uniaxial tension test in MD. (d) Poisson's ratio as a function of porosity.

carbon and are only appropriate for interactions between water and carbons in the plane of the graphene membrane.

A representative instance of NPG fracture from MD simulations is shown in Figure 2, with virial atomic stresses represented as stress times volume since atomic volumes are not always well-defined.[22] Prior to fracture, the entire membrane is in a state of plane stress with regions away from nanopores experiencing less stress than atoms located in the immediate vicinity of a nanopore. Carbon−carbon bonds colored red have buckled earlier in the simulation and are therefore in a lower state of stress. The average stress in the membrane increases as a function of strain, until a defect is nucleated (top right of Figure 2a) in the vicinity of a pore and eventually grows into a full crack. This indicates that failure in

dx.doi.org/10.1021/nl502399y | Nano Lett. 2014, 14, 6171−6178

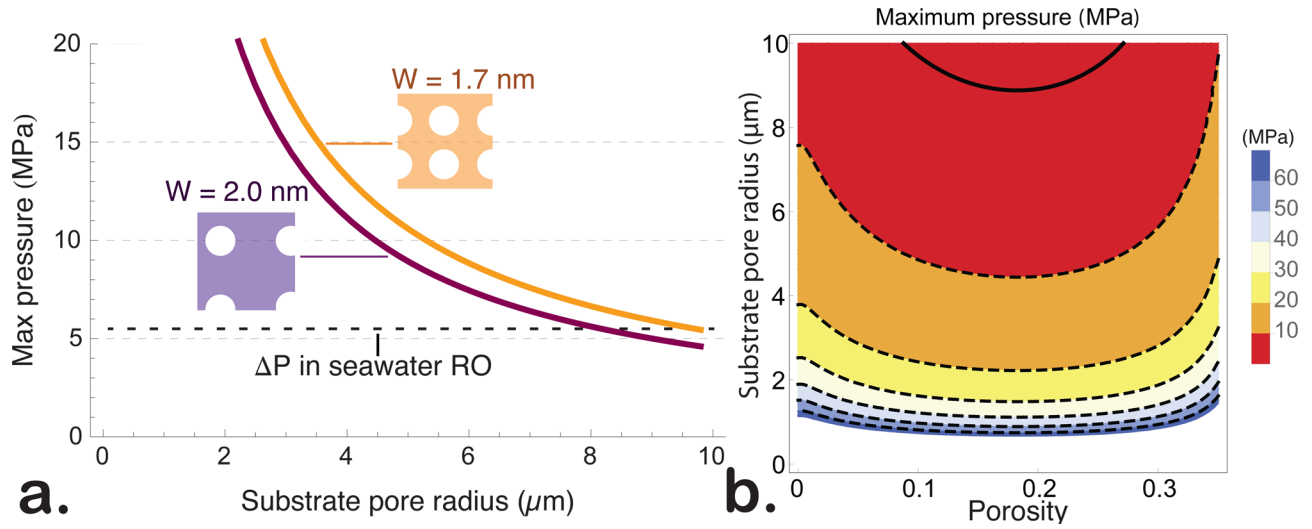

Figure 4. (a) Maximum hydraulic pressure at membrane failure as a function of substrate pore radius. An NPG membrane with pores spaced by W = 1.7 nm (orange) or 2.0 nm (purple) could withstand pressures greater than those typically employed in seawater RO (dashed line) as long as all the pores in the substrate are smaller than 8−10 μm. (b) Contour plot of maximum hydraulic pressure as a function of NPG porosity and substrate pore radius for a = 0.5 nm.

NPG is characterized by brittle fracture initiated at the nanopores.

The stress−strain curve from a typical simulation with nanopore radius a = 0.5 nm and nanopore separation W = 4.0 nm is shown in Figure 2b. The figure indicates that graphene exhibits elastic (hysteresis-free) behavior prior to fracture but that the relation between stress and strain is nonlinear for $\varepsilon >$ 3%. This observation is consistent with prior work on the mechanical properties of graphene.[8]

We have performed these MD simulations for a range of wet and dry NPG samples with varying values of nanopore size and separation, and we noted the fracture stress in each sample. For each set of conditions, up to 10 MD simulations were performed with different, uncorrelated starting configurations. In contrast with prior work, we do not find that the presence of water consistently lowers the fracture stress of graphene.[21] We discuss the influence of water on the strength of graphene in greater detail below. Given that NPG undergoes brittle fracture at sufficiently high stress, we expect from continuum mechanics that the fracture stress of NPG should decrease if its nanopores are larger or if they are spaced closer together. The critical stress intensity is related to fracture stress for an internal flaw of radius a as

$$\sigma_f = f(W)\frac{K_{IC}}{\sqrt{\pi a}} \tag{1}$$

where K_{IC} is fracture toughness of the material in tensile (mode I) loading, and $f(W)$ is a pre-factor that reflects the geometry of the test specimen including deviations from plane strain, sample thickness and width relative to the flaw dimensions, plasticity at the crack tip, and nanopore spacing.

The fracture stresses obtained from MD are shown in Figure 3a. Consistent with the continuum case, we find that σ_f decreases monotonically with nanopore size and increases with nanopore separation. We have performed linear regressions from the fracture stresses from MD at constant pore radius (a = 0.5 nm) and constant pore separation (W = 4.0 nm) to obtain the fitting parameters in eq 1, using the empirical fit $f(a,W) = (1 - \exp(-W/\alpha))$ with α = 2.6 nm, and Figure 3a,b indicates good agreement between the fitting function and the MD data. From this fitting procedure, the fracture toughness of wet NPG was found to be K_{IC} = 5.01 ± 0.03 MPa m$^{1/2}$. The fracture toughness of dry graphene, calculated using a similar fitting method and assuming the same value of α as for wet graphene, is 35% lower than that of wet graphene at 3.25 ± 0.22 MPa m$^{1/2}$, which is within 23% of previous results obtained from ab initio calculations[23] and within 19% of experimental results.[24]

Thus, nanopores in an NPG membrane behave similarly to cracks as far as their effect on fracture mechanics is concerned. This is noteworthy because previous work has shown that in contrast, 5−7 defects arising from grain boundaries in graphene do not follow the usual rules of continuum fracture mechanics.[25] We hypothesize that the reason why nanopores behave more consistently with continuum fracture mechanics is that they do not produce substantial prestrain at equilibrium, unlike grain boundary samples in which prestrain in specific bonds was identified as the main cause of early failure.[25]

We also computed the elastic properties of NPG as a function of pore radius and separation (see Figure 3c,d). Because the elastic constants of porous materials are known to depend on porosity,[26,27] we computed the biaxial elastic modulus and Poisson's ratio for each simulation, and we used a two-variable linear regression to fit the value of the elastic constants as a function of porosity $p = \pi a^2/W^2$

$$E_M = E_0 + \alpha_1 p \tag{2}$$

$$\nu = \nu_0 + \beta_1 p \tag{3}$$

The fitting parameters were found to be E_0 = 876 GPa, α_1 = −2368 GPa, ν_0 = 0.117, β_1 = 0.0496. For comparison, the experimental values for pristine graphene are $E_M \sim$ 790 GPa and ν = 0.17.[13] Our choice of fitting function is simpler than models proposed in the literature for porous ceramics,[28] yet it satisfies the necessary conditions for a suitable physical description, that is, both quantities reach zero in the limit of high porosity and converge to the pristine-graphene values in the limit of zero porosity. Figure 3d shows that ν depends only weakly on porosity and varies more from sample to sample. Given the small value of β_1 obtained from our fit and the fact

dx.doi.org/10.1021/nl502399y | Nano Lett. 2014, 14, 6171−6178

that the results in the following sections are not highly sensitive to the value of ν, our fit is relatively similar to assuming a constant value of ν. In contrast, E_M exhibits a consistent linear relationship with porosity with higher porosities corresponding to lower values of E_M.

Determining the Membrane Stress. In the previous section, we considered the fracture stress in isolation from the substrate material because the fracture stress is an intrinsic property of the NPG layer. Now, we determine the actual stress experienced by the membrane, which is relevant at the length scale of microns and depends on the substrate pore size. At this length scale, we may model the NPG as a homogeneous material suspended over substrate pores.[11] Assuming that the membrane is clamped at the substrate pore edges (a valid assumption given that graphene is known to adhere strongly to rough substrates[29]) and that no residual stress exists prior to loading, the membrane stress is expressed as

$$\sigma = \left(\frac{2}{3}\frac{E_M}{1.026 - 0.793\nu_M - 0.233{\nu_M}^2}\right)^{1/3}\left(\frac{\Delta P R}{4d}\right)^{2/3} \quad (4)$$

where E_M and ν are the Young's modulus and Poisson's ratio of the membrane, R is the substrate pore radius, and ΔP is the applied pressure (see Supporting Information for a derivation of Eq 4). For a substrate pore radius of 1 μm and ΔP = 5 MPa (which is a typical applied pressure in seawater RO operations[30]), the macroscopic membrane stress is about 5 GPa. Especially noteworthy is the fact that σ increases monotonically with E_M. This dependence implies that for a given ΔP, two membranes with different elastic moduli will experience different stresses.

Maximum Pressure in NPG. Drawing from the results above, we have calculated the maximum pressure that NPG could withstand, ΔP_{max}, as a function of substrate pore size and pore separation (see Figure 4a). As expected from eq 1, ΔP_{max} decreases monotonically with R. In particular, NPG is capable of withstanding a typical RO pressure (5 MPa) as long as $R <$ ~8 μm. Figure 4a also indicates the importance of porosity with the curve shifting to the left as W increases from 1.7 to 2 nm (or equivalently, as p decreases from 21% to 9% respectively). In order to elucidate the combined effect of porosity and substrate pore size on ΔP_{max}, we have also plotted ΔP_{max} in a contour plot with p on the y-axis and R on the x-axis in Figure 4b. The solid black line delimits acceptable combinations of R and p from those that would result in fracture at ΔP = 5 MPa.

A surprising result is that the maximum pressure can in some cases increase as a function of porosity, even though we have shown above that the fracture stress of NPG decreases with greater porosity. This is indicated by the fact that ΔP_{max} exhibits a minimum for $p \sim$ 15−20% in Figure 4b. A closer examination reveals the reason underlying this phenomenon. Figure 3 showed that greater porosity lowers the fracture stress of the membrane, but also that it decreases its elastic modulus. Because $\sigma \propto E_M^{1/3}$ (see previous section), the membrane stress also decreases with greater porosity. Thus, there is a competition between decreasing fracture stress and decreasing membrane stress as porosity increases, as indicated in Figure 5.

The figure shows that as porosity increases from 0 to ~10%, σ_f drops below the value of σ, meaning that the membrane becomes unable to withstand the applied pressure. This crossover would also occur even if σ did not vary with E_M (dashed line in the figure). But as p continues to increase from 10%, σ steadily decreases until it crosses σ_f again at p = 27%.

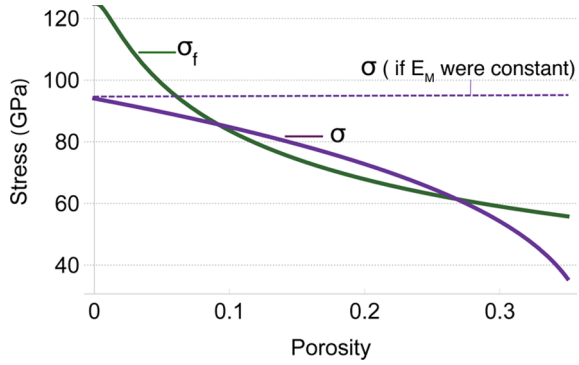

Figure 5. Fracture stress σ_f (green) and membrane stress σ (purple) as a function of porosity for a = 0.5 nm, ΔP = 5.5 MPa, and R = 9 μm. The dashed line indicates the membrane stress if E_M were constant (E_M = 790 GPa) instead of evolving with porosity.

For $p >$ 27%, the membrane stress is again lower than the fracture stress, indicating a region of mechanical stability. In other words, the NPG system exhibits an unusual mechanical behavior in which the membrane can withstand higher pressures when its porosity increases. We attribute this behavior to the mixed boundary conditions imposed on the membrane, which account for the E_M dependence in the expression for σ. This is because the membrane is clamped at the edges but is still allowed to bulge out of plane. Although the unusual behavior described here is not inherently specific to NPG, the implications of greater pressure resilience at higher porosity have received little attention to date. For example, recent work on the mechanics of microfiltration supported over square-shaped holes drew similar relationships between E_M and p on the one hand, and P_{max} and E_M on the other, although the influence of p on P_{max} was not addressed.[31] Having established how the morphology of the NPG and substrate layers determine the membrane's mechanical resilience, we discuss in the remaining paragraphs the implications of hydraulic pressure on the desalination performance of an NPG membrane and the effects of water and crystal imperfections on NPG strength.

Effect of Pressure on Desalination Performance. While this paper primarily examines the mechanical strength of an NPG membrane, we also note that high hydraulic pressures have an effect on the desalination performance of the membrane. Because of its exceptional elastic properties, graphene can withstand ~20% strain prior to fracture, as indicated in Figure 2b. This amount of strain may directly affect RO performance, because the salt rejection in an NPG membrane is highly sensitive to nanopore size.[3] In order to quantify this effect to first order, we have estimated the change in water permeability and salt rejection that results when an NPG membrane is strained (see Figure 6). The methodological details are given in the Supporting Information.

The figure indicates that higher pressures produce additional strain in the nanopores, which results in greater permeability (Figure 6a) but worse salt rejection (Figure 6b). The white region in the top-right corner of each plot indicates the combinations of a and ΔP that would result in NPG fracture, that is, $\sigma \geq \sigma_{max}$. The fact that the contour lines in both plots are curved as opposed to vertical suggests that the applied pressure has a non-negligible effect on the desalination properties of NPG. For example, we find that increasing ΔP

dx.doi.org/10.1021/nl502399y | Nano Lett. 2014, 14, 6171−6178

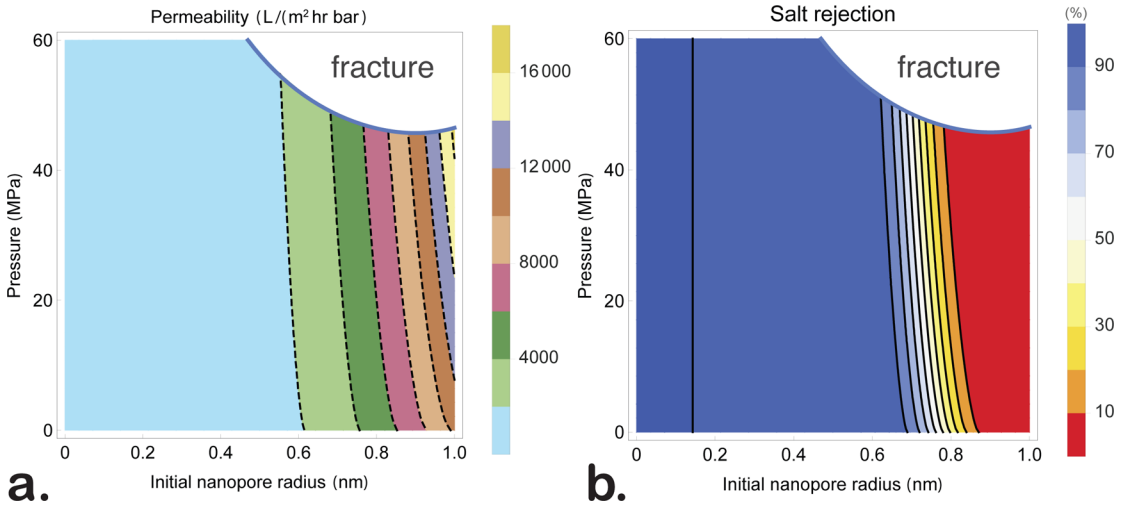

Figure 6. Contour plots of water (a) permeability (in L/m^2-hr-bar) and (b) salt rejection (in %) of NPG as a function of initial nanopore size (x-axis) and applied pressure (y-axis).

from 1 to 5 MPa enhances the permeability of NPG by about 5%.

Effect of Water and Grain Boundaries. Our MD results indicate that the presence of water affects the fracture toughness of graphene with dry samples withstanding about 35% lower stresses than wet samples. To understand this effect, we note that the fracture toughness of graphene can be expressed as $K_{IC} = (2\gamma E_M/d)^{1/2}$, where γ is the free edge energy.[24] Because graphene is hydrophobic, there is an additional energy penalty for creating new edges in the presence of water, which results in a higher γ and therefore a larger K_{IC}. To verify this, we have calculated the free edge energy of graphene in the presence and absence of water (see Supporting Information). Consistent with our hypothesis, we found that the free edge energy of wet graphene (γ_{wet} = 1.33 eV/Å) is larger than that of dry graphene (γ_{dry} = 1.16 eV/Å, which is consistent with previous computational work[24]). Because the graphene edges in our simulation are hydrophobic, there is an additional energy penalty for creating new edges in the presence of water, which results in a higher γ and therefore a larger K_{IC}. To verify this, we have calculated the free edge energy of graphene in the presence and absence of water (see Supporting Information). Consistent with our hypothesis, we found that the free edge energy of wet graphene (γ_{wet} = 1.33 eV/Å) is larger than that of dry graphene (γ_{dry} = 1.16 eV/Å), which is consistent with previous computational work.[32] This indicates that the greater fracture strength of wet graphene relative to dry graphene in our simulations is related to the difference in free energy of wet vs dry graphene edges. Although the graphene edges in our simulations were unsaturated, we note that the value we have obtained for γ_{dry} lies within the range of experimental values in vacuum, which is 1.0−1.4 eV/Å.[33] This suggests that our simulation approach provides appropriate estimates of edge energies even though the simulated edges are unsaturated. However, the large experimental range of values for γ_{dry} also suggests that while the mechanical properties of a graphene membrane in a given chemical environment will follow the trends demonstrated in this article, the relative strength of wet vs dry graphene may vary depending on the chemical environment and the hydrophobic or hydrophilic nature of the graphene edges. We also note that the water molecules in our computational system were not allowed to chemically react with the graphene atoms, and that simulations in which the water molecules were allowed to directly react with the graphene as it is being fractured would be an important consideration for future work.

Finally, we note that the presence of grain boundary defects in the membrane is unlikely to reduce the fracture strength from the GPa to MPa levels. Previous work has shown fracture stress of polycrystalline graphene is at least 70 GPa.[25,35] Thus, although it is possible that interactions among nanopores and grain boundaries may together reduce the fracture strength below that predicted in this study, it appears likely that polycrystalline nanoporous graphene will withstand the 5−10 MPa of applied pressure anticipated for desalination applications. Additionally, this work has also highlighted how the mechanical integrity of the membrane depends critically on the size of the substrate pores. Above ∼8 μm, the applied stress distributed across the membrane begins to reach the intrinsic breaking strength of graphene and may compromise the integrity of the membrane.

Conclusion. While ultrapermeable membranes offer considerable promise for the future of clean water technology, the results presented above demonstrate that mechanical strength and choice of substrate will be critical parameters in the design of a functioning membrane. We find that NPG is indeed capable of withstanding the hydraulic pressures involved in RO. A surprising result is that greater membrane porosity can in some cases allow for a higher maximum pressure due to the effect of porosity on the elastic modulus. While previous work had paved the way in exploring the relationship between maximum pressure and substrate morphology for NPG,[7,8] our results further indicate that the relationship between porosity and Young's modulus in NPG cannot be neglected when estimating the membrane's overall mechanical resilience.

Although we expect that laboratory experiments will eventually also be capable of empirically testing the mechanical strength of NPG, graphitryne, 2D-polyphenylene, and other proposed ultrapermeable membranes, the computational results presented here can offer important design principles. For example, applying the same methodology to graphitryne based on the results of Lin et al.[36] suggests that graphitryne (σ_{max} = 32 GPa) would fracture at lower pressures than NPG. Specifically, the maximum pressure for a graphitryne membrane supported

dx.doi.org/10.1021/nl502399y | Nano Lett. 2014, 14, 6171−6178

over 3 μm substrate pores is only 4.1 MPa, which is less than the pressure employed in seawater RO. Future work should also examine the role of membrane fouling, because it is known that fouling can significantly increase the cost of desalination.[30] In this regard, one potential advantage of graphene is that the relative resistance of graphitic carbon to chlorine[37] may facilitate the prevention of fouling by disinfection.

While the focus of this work is on the use of NPG for RO desalination, it should be noted that the mechanical properties of graphene membranes are of special relevance for a host of other applications. Of particular interest is the use of NPG as a gas separation membrane.[38,39] An NPG membrane for gas separation would likely also lie atop a porous substrate, so the approach employed here could be extended to examine the mechanical resilience of NPG in a gas separation assembly. Here, it will suffice to mention that the pressures employed in gas separations are typically lower than those employed for RO, so NPG should also able to withstand gas separation pressures in most cases. Graphene has also been proposed for the fabrication transparent graphene electrodes for touch-screen displays,[40,41] and graphene oxide has also been incorporated into ultrafiltration membranes for water purification.[42] The mechanical resilience of graphene will also play a critical role in these applications.

In the case of RO, our results suggest that a redesign of the membrane substrate may still be desirable. A statistical analysis of substrate pore sizes in polysulfone by Nakao et al. suggests an average substrate pore radius of 0.2 μm with few or no pores larger than 2.5 μm.[43] But while the polysulfone chemistry employed in TFC membranes contains features that are nominally in the 100 nm range, the inherently stochastic distribution of substrate pore sizes in the material makes it possible that several substrate pores in a 40 m^2 membrane sheet would extend wider than ~8 μm. By altering the polymer chemistry of the substrate, it could be become possible to ensure that the entire NPG membrane maintains its mechanical stability. Thus, an NPG membrane over a substrate with pores no greater than 1 μm would be expected to withstand hydraulic pressures upward of 57 MPa, nearly 10 times higher than in typical seawater RO operations today.

■ ASSOCIATED CONTENT

Supporting Information

Supplementary figures and associated captions. This material is available free of charge via the Internet at http://pubs.acs.org.

■ AUTHOR INFORMATION

Corresponding Author

*E-mail: jcg@mit.edu.

Author Contributions

The manuscript was written through contributions of all authors. All authors have given approval to the final version of the manuscript.

Notes

The authors declare no competing financial interest.

■ ACKNOWLEDGMENTS

We thank Michael Demkowicz, John Maloney, Krystyn Van Vliet, Shreya Dave, Yun Liu, Alexie Kolpak, Amanda Evans, Andrey Zarur, Rajamani Raghunathan, Jeong Yun Kim, Jason Sia, Ándras Kovács, and the Grossman Group for insightful conversations. We gratefully recognize NERSC for computational resources. Funding sources are the Doug C. Spreng Fund, Deshpande Center, NSF Graduate Research Fellowship Program, and the Martin Family Sustainability Fellowship.

■ ABBREVIATIONS

NPG, nanoporous graphene; NPG, hydrogenated nanoporous graphene; MD, molecular dynamics; RO, reverse osmosis

■ REFERENCES

(1) Elimelech, M.; Phillip, W. A. *Science* **2011**, *333*, 712−717.
(2) Addams, L.; Boccaletti, G.; Kerlin, M.; Stuchtey, M.; McKinsey and Company. *Charting Our Water Future: Economic Frameworks to Inform Decision-making*; 2030 Water Resources Group: 2009.
(3) Cohen-Tanugi, D.; Grossman, J. C. *Nano Lett.* **2012**, *12*, 3602−3608.
(4) Konatham, D.; Yu, J.; Ho, T. A.; Striolo, A. *Langmuir* **2013**, 11884−11897.
(5) Cohen-Tanugi, D.; McGovern, R. K.; Dave, S. H.; Lienhard, J. H. V.; Grossman, J. C. *Energy Environ. Sci.* **2014**, *7*, 1134.
(6) Young, W.; Budynas, R.; Sadegh, A. *Roark's Formulas for Stress and Strain*, 8th ed.; McGraw-Hill Professional: New York, 2011.
(7) Liu, Y.; Chen, X. *J. Appl. Phys.* **2014**, *115*, 17A715.
(8) Song, Z.; Xu, Z.; Huang, X.; Kim, J.-Y.; Zheng, Q. *J. Appl. Mech.* **2013**, *80*, 040911.
(9) Takuji, O.; Mitsuo, K.; Takeshi, M. *Eng. Fract. Mech.* **1994**, *48*, 137−146.
(10) Kahler, B.; Swain, M. V.; Moule, A. *J. Biomech.* **2003**, *36*, 229−237.
(11) Schomburg, W. K. *Introduction to Microsystem Design*; Springer: New York, 2011.
(12) Baker, R. *Membrane Technology and Applications*, 2nd ed.; Wiley: New York, 2004.
(13) Lee, C.; Wei, X.; Kysar, J. W.; Hone, J. *Science* **2008**, *321*, 385−388.
(14) Ghosh, A. K.; Hoek, E. M. V. *J. Membr. Sci.* **2009**, *336*, 140−148.
(15) Singh, P. S.; Joshi, S. V.; Trivedi, J. J.; Devmurari, C. V.; Rao, A. P.; Ghosh, P. K. *J. Membr. Sci.* **2006**, *278*, 19−25.
(16) McCutcheon, J. R.; Elimelech, M. *J. Membr. Sci.* **2008**, *318*, 458−466.
(17) Kim, H. I.; Kim, S. S. *J. Membr. Sci.* **2006**, DOI: 10.1016/j.memsci.2006.09.037.
(18) Min, K.; Aluru, N. R. *Appl. Phys. Lett.* **2011**, *98*, 013113−013113−3.
(19) Humphrey, W.; Dalke, A. *Journal of Molecular Graphics* **1996**, DOI: 10.1016/0263-7855(96)00018-5.
(20) Plimpton, S. *J. Comput. Phys.* **1995**, *117*, 1−19.
(21) Wong, C. H.; Vijayaraghavan, V. *Mater. Sci. Eng., A* **2012**, *556*, 420−428.
(22) Costescu, B. I.; Frauke, G. *Physical Chemistry Chemical Physics* **2014**, *16*, 12582.
(23) Xu, M.; Tabarraei, A.; Paci, J. T.; Oswald, J.; Belytschko, T. *Int. J. Fract.* **2012**, *173*, 163−173.
(24) Zhang, P.; Ma, L.; Fan, F.; Zeng, Z.; Peng, C.; Loya, P. E.; Liu, Z.; Gong, Y.; Zhang, J.; Zhang, X.; Ajayan, P. M.; Zhu, T.; Lou, J. *Nat. Commun.* **2014**, *5*, 3782.
(25) Grantab, R.; Shenoy, V. B.; Ruoff, R. S. *Science* **2010**, *330*, 946−948.
(26) Lam, D. C. C.; Lange, F. F.; Evans, A. G. *J. Am. Ceram. Soc.* **1994**, *77*, 2113−2117.
(27) Kováčik, J. *J. Mater. Sci.* **2006**, *41*, 1247−1249.
(28) Kováčik, J. *J. Mater. Sci. Lett.* **1999**, *18*, 1007−1010.
(29) Koenig, S. P.; Boddeti, N. G.; Dunn, M. L.; Bunch, J. S. *Nat. Nanotechnol.* **2011**, *6*, 543−546.
(30) Fritzmann, C.; Löwenberg, J.; Wintgens, T.; Melin, T. *Desalination* **2007**, *216*, 1−76.
(31) Kovács, A.; Kovács, A.; Pogány, M.; Mescheder, U. *Sens. Actuators, B* **2007**, *127*, 120−125.
(32) Zhang, X.; Xin, J.; Ding, F. *Nanoscale* **2013**, *5*, 2556−2569.

(33) Gao, J.; Zhao, J.; Ding, F. *J. Am. Chem. Soc.* **2012**, *134*, 6204−6209.
(34) Liu, Y.; Dobrinsky, A.; Yakobson, B. I. *Phys. Rev. Lett.* **2010**, *105*, 235502.
(35) Lee, G.-H.; Cooper, R. C.; An, S. J.; Lee, S.; van der Zande, A.; Petrone, N.; Hammerberg, A. G.; Lee, C.; Crawford, B.; Oliver, W. *Science* **2013**, *340*, 1073−1076.
(36) Lin, S.; Buehler, M. J. *Nanoscale* **2013**, *5*, 11801−11807.
(37) Wendt, H.; Dermeik, S.; Ziogas, A. *Mater. Corros.* **1990**, *41*, 457−463.
(38) Koenig, S. P.; Wang, L.; Pellegrino, J.; Bunch, J. S. *Nat. Nanotechnol.* **2012**, *7*, 728−732.
(39) Ambrosetti, A.; Silvestrelli, P. L. *J. Phys. Chem. C* **2014**, *118*, 19172−19179.
(40) Chen, H.; Chen, H.; Müller, M. B.; Müller, M. B.; Gilmore, K. J.; Gilmore, K. J.; Wallace, G. G.; Wallace, G. G.; Li, D.; Li, D. *Adv. Mater.* **2008**, *20*, 3557−3561.
(41) Kim, K. S.; Kim, K. S.; Zhao, Y.; Zhao, Y.; Jang, H.; Jang, H.; Lee, S. Y.; Lee, S. Y.; Kim, J. M.; Kim, J. M.; Kim, K. S.; Kim, K. S.; Ahn, J.-H.; Ahn, J.-H.; Kim, P.; Kim, P.; Choi, J.-Y.; Choi, J.-Y.; Hong, B. H.; Hong, B. H. *Nature* **2009**, *457*, 706−710.
(42) Wang, Z.; Yu, H.; Xia, J.; Zhang, F.; Li, F.; Xia, Y.; Li, Y. *Desalination* **2012**, *299*, 50−54.
(43) Nakao, S.-I. *J. Membr. Sci.* **1994**, *96*, 131−165.